AD-A095 474 COLD REGIONS RESEARCH AND ENGINEERING LAB HANOVER NH F/G 8/12
ICING ON STRUCTURES.(U)
DEC 80 L D MINSK
UNCLASSIFIED CRREL-80-31 NL

1 OF 1
AD A
095474

END
DATE
FILMED
3-81
DTIC

CRREL

Icing on structures

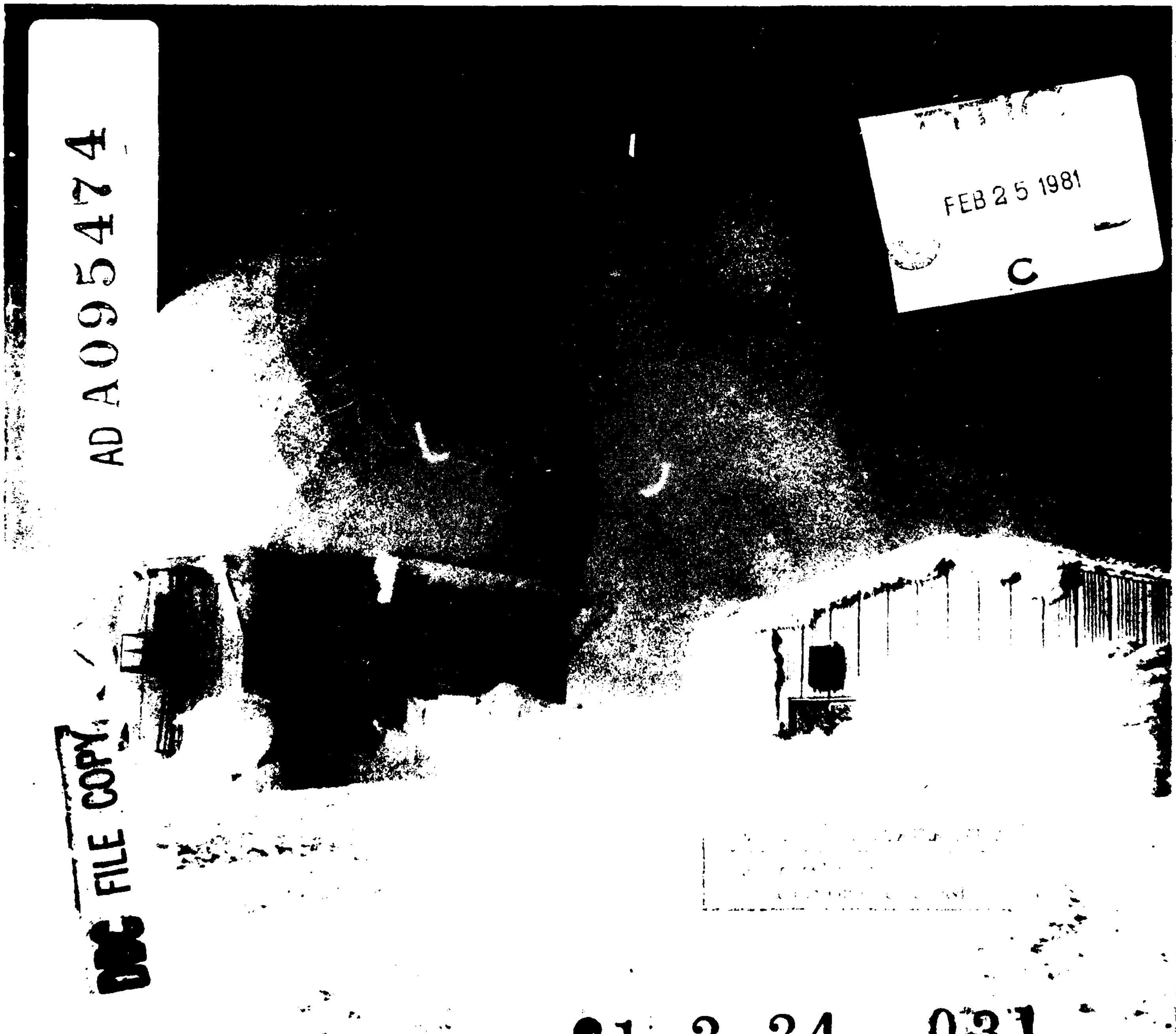

Cover: Mountain-top radar site in Alaska encrusted with rime accumulation. (Photograph by author.)

CRREL-[redacted]t 80-31

Icing on structures,

L.D. Minsk

Dec[redacted]980

Prepared for
OFFICE OF MARINE GEOLOGY
U.S. GEOLOGICAL SURVEY
By
UNITED STATES ARMY
CORPS OF ENGINEERS
COLD REGIONS RESEARCH AND ENGINEERING LABORATORY
HANOVER, NEW HAMPSHIRE, U.S.A.

Unclassified

SECURITY CLASSIFICATION OF THIS PAGE *(When Data Entered)*

REPORT DOCUMENTATION PAGE		READ INSTRUCTIONS BEFORE COMPLETING FORM
1. REPORT NUMBER CRREL Report 80-31	2. GOVT ACCESSION NO. AD-A095 474	3. RECIPIENT'S CATALOG NUMBER
4. TITLE *(and Subtitle)* ICING ON STRUCTURES		5. TYPE OF REPORT & PERIOD COVERED
		6. PERFORMING ORG. REPORT NUMBER
7. AUTHOR(s) L.D. Minsk		8. CONTRACT OR GRANT NUMBER(s)
9. PERFORMING ORGANIZATION NAME AND ADDRESS U.S. Army Cold Regions Research and Engineering Laboratory Hanover, New Hampshire 03755		10. PROGRAM ELEMENT, PROJECT, TASK AREA & WORK UNIT NUMBERS
11. CONTROLLING OFFICE NAME AND ADDRESS Office of Marine Geology U.S. Geological Survey Reston, Virginia 22092		12. REPORT DATE December 1980
		13. NUMBER OF PAGES 22
14. MONITORING AGENCY NAME & ADDRESS*(if different from Controlling Office)*		15. SECURITY CLASS. *(of this report)* Unclassified
		15a. DECLASSIFICATION/DOWNGRADING SCHEDULE

16. DISTRIBUTION STATEMENT *(of this Report)*

Approved for public release; distribution unlimited.

17. DISTRIBUTION STATEMENT *(of the abstract entered in Block 20, if different from Report)*

18. SUPPLEMENTARY NOTES

19. KEY WORDS *(Continue on reverse side if necessary and identify by block number)*

Deicing materials
Deicing systems
Ice
Ice accretion
Ice loads
Ice prevention

20. ABSTRACT *(Continue on reverse side if necessary and identify by block number)*

Ice accretion on structures built on the earth's surface is discussed. Sources of water are the atmosphere or water bodies near or surrounding the structure. Ice types include frost, rime, glaze, and spray; properties and conditions governing their formation are presented. Methods of estimating accretion rates and total accretion on structures are given, and extracts from U.S. and Canadian codes for ice and wind loads on structures are included. Techniques for preventing or removing ice accretion are presented.

PREFACE

This report was prepared by L. David Minsk, Research Physical Scientist, Applied Research Branch, Experimental Engineering Division, U.S. Army Cold Regions Research and Engineering Laboratory.

The report was prepared for the Office of Marine Geology, U.S. Geological Survey.

Technical reviewers of the report were John M. Sayward and Stephen F. Ackley of CRREL.

CONTENTS

ILLUSTRATIONS

TABLES

ICING ON STRUCTURES

L.D. Minsk

1. Types of ice accretion

Ice formation on a surface exposed to the atmosphere can occur in one of two ways: by flooding of the surface by a large volume of water or by accretion of discrete water "particles." Flooding of a surface and the subsequent freezing of a ponded volume applies only to a horizontal surface. We are concerned with the process of ice formation on both vertical and horizontal surfaces, and therefore this discussion will be confined to droplet or particle accretion processes. The two sources of liquid particles are atmospheric processes (which produce hydrometeors) and wind shear of, or splashing from the surface of, a large body of water (droplets arising from this source are also frequently considered hydrometeors). Atmospheric sources result in the formation of frost, rime, or glaze, whereas spray sources can result only in the formation of rime or glaze. Characteristics of icing sources are listed in Table 1.

a. Frost

Water vapor in the air may deposit on a surface which is at or below 0°C to form frost, or more properly "hoarfrost" (*hoar* is the generic term for ice crystals formed directly from the vapor phase). Hoarfrost can form only when the air is still or very nearly so. The resulting bond between the crystal and accreting surface ranges from very strong (e.g. frost formed on house windows or on automobile windshields) to very weak (e.g. surface hoar formed on a snow surface or on road pavement). The growth of hoarfrost is limited by the amount of water vapor in the air; since there is little vapor at subfreezing temperatures, the total amount accumulating on an exposed surface is small compared to other types of ice accretion. Therefore we will not consider frost further.

b. Rime

Discrete water droplets in the atmosphere can easily become supercooled because of their small volume. When the supercooled droplets strike a surface they will freeze as soon as the latent heat of fusion is dissipated. Hard rime will form when the heat loss is relatively slow, allowing "wet growth" to occur whereby some flow of freezing droplets can occur before complete crystallization. Soft rime forms when droplets freeze very rapidly upon deposition, resulting in characteristic granular structure. Hard rime is the denser and harder of the two; its density ranges between 0.1 and 0.6 Mg/m^3, in contrast to 0.01-0.08 Mg/m^3 for soft rime. Hard rime appears milky or translucent, depending on the amount of air trapped within the structure. Soft rime, because of its much lower density, is more delicate in structure and can appear quite fluffy, though lamellar and needle-like forms also exist. Rime grows principally into the wind, as individual small water droplets impinge one on top of another after coating an accreting surface.

c. Glaze

When the water droplets striking a surface have sufficient time to flow in a continuous film over the accreting surface prior to freezing, a hard, nearly homogeneous ice is formed called glaze ice (or "glare ice" or "black ice," because of its characteristic specular reflection of light). Because the surface has been wetted nearly completely prior to freezing, a very strong bond results. It is generally bubble-free, and

Table 1. Characteristics of icing sources.

Source	Droplet diameter range (μm)	Mean droplet diameter (μm)	Liquid water content (g/m^3)	Droplet concentration per cm^3	Reference
Sea spray					
Breaking waves	1000-3500	2400	4600		Borisenkov and Panov (1972)
Wave crests	60-1000	*(150-200)*			Borisenkov and Panov (1972) (Wu 1973)
Fog					
Advection	6-64	20	0.17	40	Kocmond et al. (1971)
Radiation	4-36	10	0.11	200	Kocmond et al. (1971)
"Sea fog"	?-120	46	0.13		Houghton and Radford (1938)
Cloud					
Stratus	1.5-43	4.9	(0.05-0.25)		Pilié and Kocmond (1967) (Borovikov et al. 1961)
Cumulus (cumulonimbus)	4-200	40	2.5	72	Weickmann and aufm Kampe (1953)

Table 2. Types of ice from atmospheric sources.

Type of ice	Appearance	Density (Mg/m^3)	Conditions of formation
Glaze	A hard, well-bonded, generally clear homogeneous ice	0.7-0.9	Supercooled water droplets at a temperature close to freezing (0° to −3°C) and wind speeds of 1-20 m/s
Hard rime	A hard, granular white or translucent ice growing in the direction of the wind	0.1-0.6	Supercooled water droplets at a temperature of −3° to −8°C, wind speeds generally 5-10 m/s
Soft rime	A white, opaque, granular ice with delicate structure only loosely bonded, growing in the direction of the wind	0.01-0.08	Supercooled water droplets at a temperature of −5° to −25°C and low wind speed (1-5 m/s)

therefore its density approaches that of bubble-free ice (0.917 Mg/m^3 or 57.3 lb/ft^3). It is also very hard. The crushing strength of bulk ice was determined by Butkovich (1954) (Fig. 1). The degree to which ice is bonded to a substrate is measured in terms of the interfacial shear strength. Generally, the lower the temperature, the higher the shear strength. The difference in coefficients of thermal expansion between ice and materials to which it is bonded is one reason for the widely varying values reported in the literature.

A summary of ice formed from atmospheric sources is given in Table 2.

d. Spray ice

Droplets can be generated by breaking waves, by the shattering of trapped air bubbles as they rise to the surface of the water, and by wind forces. But the splashing of waves against an object in the water (such as a ship hull or a fixed structure) produces the most and largest droplets. Only an insignificant amount of water from spray sources has been measured higher than 16 m (52.5 ft) above the waterline on a ship (Anon. 1962). Spray ice orginating from seawater will generally include brine pockets, since salts must be rejected before the ice will freeze at 0°C, and the increasing concentration of the brine may depress its freezing point well below the ambient temperature. Sea spray ice, therefore, is weaker than freshwater ice, but it may adhere just as strongly to a surface when no brine pockets are present at the interface.

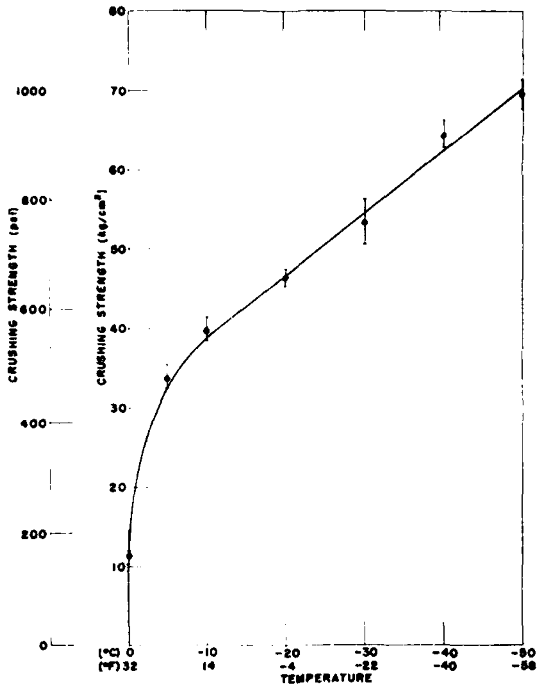

Figure 1. Crushing strength vs temperature for commercial artificial ice. Load applied normal to long axis of prismatic crystals (Butkovich 1954).

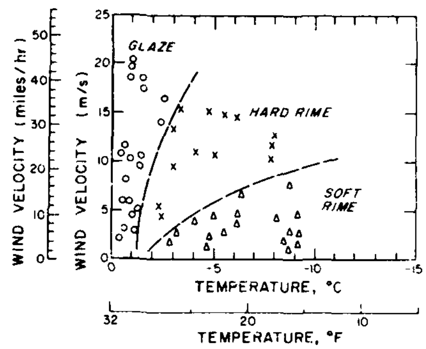

Figure 2. Relationship between meteorological conditions and type of icing (Kuroiwa 1965).

2. Conditions governing type of accreted ice

a. Meteorological

Since ice forms by the accretion of cold or supercooled water droplets which must dissipate their heat of fusion, the type of ice that results will be governed by the temperature of the droplets and their size, as well as the rate at which they strike the surface. The factors governing this rate are the wind speed and the number of droplets in a unit volume, i.e. the liquid water content (LWC). The air temperature is also important in two respects: in its influence on the rate of heat dissipation by convection to the surrounding air, and its possible influence on the temperature of the accreting surface. That air temperature in itself is not a strong indicator of an icing condition is suggested by observations of glaze ice formation at surface air temperatures as low as -20°C (-4°F) and as high as 5°C (41°F), though this type of ice occurs most frequently between -3 and 0°C (27 and 32°F). Kuroiwa (1965), however, has shown that the type of ice can be correlated with three wind velocity-air temperature regimes and three air temperature-droplet diameter regimes, in observations made on Mt. Fuji (alt. 3776 m) and Mt. Neseko (alt. 1300 m) in Japan. The graph in Figure 2 illustrates the general principle that under conditions of high wind speeds and air temperatures and large droplet sizes, glaze ice will predominate because flow of the impacting drops can occur prior to freezing, and most or all air can be excluded. At the other extreme, when wind speeds and air temperatures are low and droplets small, soft rime will predominate, because of the rapid freezing of the more supercooled droplets upon impact before any flow can take place. Thus, considerable air can be entrained in the ice, resulting in its characteristically low bulk density. In between these extremes hard rime will form. It will still exhibit a grainy structure, but some flow will have taken place, excluding some air.

The liquid water content varies with the type of cloud; in fact, this is one of the principal determinants of cloud type. Ice accretion should therefore bear some relationship to the cloud type present during ice formation. Glukhov (1972) has shown this relationship from data obtained from a 300-m-high instrumented tower in the Soviet Union (Tables 3 and 4).

b. Structural

The type of ice formed is not influenced strongly by the structure itself, though the amount and shape of the ice accretion will depend upon the structure's geometry and exposure. A rigid, fixed cylinder will retain a fixed

Table 3. **Relative frequency of types of ice formed according to cloud type (%) (Glukhov 1972).**

Cloud type	Glaze	Hard rime	Soft rime	Mixture	No. of observations
	Type of ice accretion				
Stratus (St)	18	48	4	30	227
Stratocumulus (Sc)	6	66	–	28	75
Nimbostratus (Ns)	28	36	–	36	89
Fractonimbus (Frnb)	26	33	6	35	65

Table 4. **Relative frequency of ice accretion according to cloud type and air temperature (%) (Glukhov 1972).**

Cloud Type	Air temperature (°C) 0.0 -2.0	-2.1 -4.0	-4.1 -6.0	-6.1 -8.0	-8.1 -10.0	-10.1 -12.0	-12.1 -14.0	No. of observations
Stratus (St)	30	16	16	11	15	10	2	227
Stratocumulus (Sc)	14	8	31	24	13	5	5	78
Nimbostratus (Ns)	52	28	10	5	3	1	1	92
Fractonimbus (Frnb)	47	19	19	9	6	—	—	65

orientation into the wind, and droplets striking the windward side cannot cause accretion on the le ward side unless water flows there. Thus rime will ' rm only into the wind–the lee side will remain ice-free Glaze ice, however, may form both on the windward and leeward sides when flow takes place around the cylinder. In strong winds, a "tail" or plume of ice may be driven by viscous flow around the cylinder. If the accreting cylinder is free to rotate, as is the case with guy wires, some antennas, and transmission lines, gravitational forces acting on the accretion on the windward side may cause the cable to rotate, exposing a fresh surface for accretion. Thus, a cylindrical deposit will build up, and the type of ice resulting may be shifted if the conditions are on the borderline between two of the three growth regimes.

3. Accretion rates

a. Fundamentals

The amount of ice deposited on a unit length of cylinder in unit time is given by

$$dM/dt = 2REVw \quad (1)$$

where M = mass of droplets causing icing in time t, g
R = cylinder radius, m
E = collection efficiency, $0 \leq E \leq 1$
V = wind speed, m/s
w = cloud liquid water content, g/m^3

Not all droplets in the volume of air equivalent to the projected area of the accreting surface will strike the surface, and of those doing so some may not freeze but will be blown off. The collection efficiency accounts for this; if all droplets in the airstream strike and freeze on the surface, $E = 1$, whereas any loss is reflected in $E < 1$. E is defined as the ratio of the mass of water droplets striking the surface in unit time to the mass of droplets which would have struck the surface if they had not been deflected (see Fig. 3). According to Langmuir and Blodgett (1946), E is a function of two parameters, K and Φ:

$$\left.\begin{aligned} K &= 1.29 \times 10^3\,(Vr^2/R) \\ \text{and} \quad \Phi &= 0.175\,VR \end{aligned}\right\} \quad (2)$$

(for sea level and 0°C conditions), where r = droplet radius (cm), V = wind speed (cm/s), and R = cylinder radius (cm).

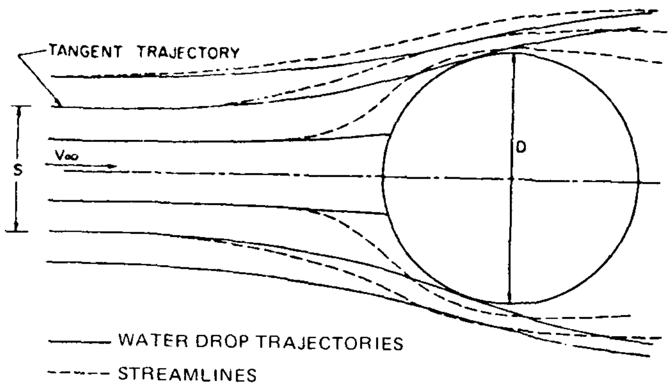

Figure 3. Collection efficiency of a cylinder. Water droplets following trajectories off the center line approach will be deflected and, at a certain distance from the axis, will not impinge on the cylinder. Collection efficiency is the ratio of the mass of droplets striking the cylinder to the total mass that would impinge if they were not deflected. If a constant mass flux is assumed, this can be represented in terms of the linear measures S and D, so that E = S/D (Stallabrass and Hearty 1967).

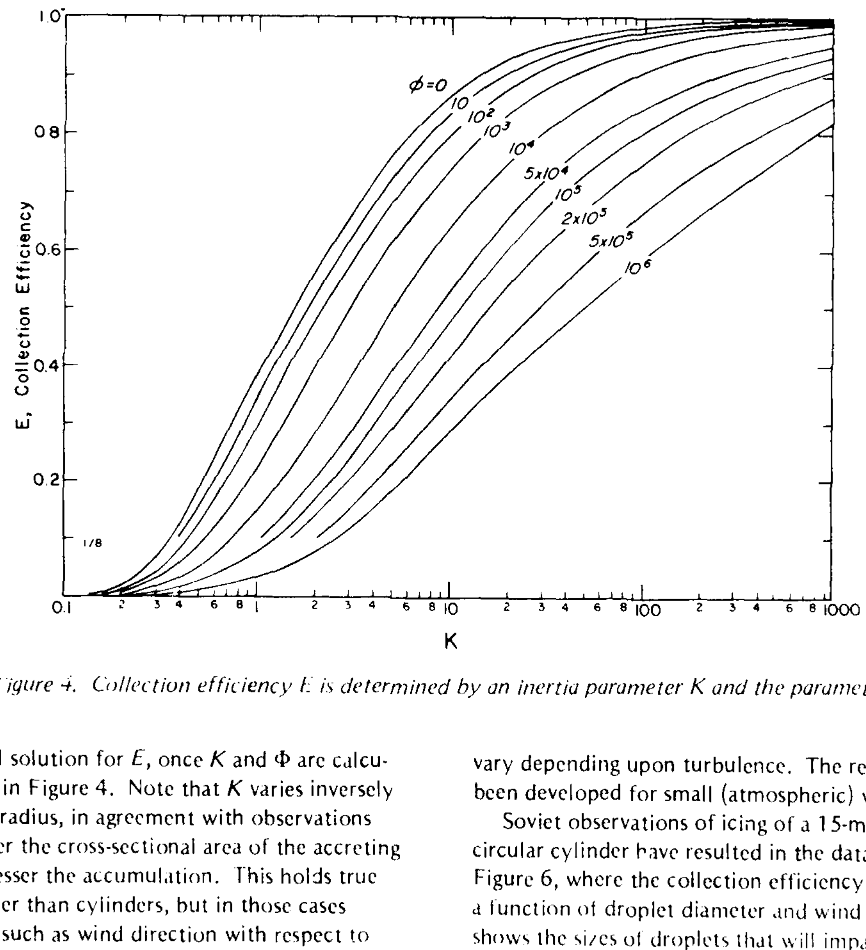

Figure 4. Collection efficiency E is determined by an inertia parameter K and the parameter Φ.

A graphical solution for E, once K and Φ are calculated, is given in Figure 4. Note that K varies inversely with cylinder radius, in agreement with observations that the greater the cross-sectional area of the accreting cylinder the lesser the accumulation. This holds true for shapes other than cylinders, but in those cases other factors, such as wind direction with respect to the surface, become important. If $K < 1/8$, $E = 0$ for any Φ. Manipulation of these equations can give the critical radius of a cylinder above which icing theoretically will not take place. A graphical solution is given in Figure 5. The actual size of the cylinder will vary depending upon turbulence. The relationship has been developed for small (atmospheric) water droplets.

Soviet observations of icing of a 15-mm-diameter circular cylinder have resulted in the data plotted in Figure 6, where the collection efficiency E is given as a function of droplet diameter and wind speed. This shows the sizes of droplets that will impact on a cylinder at a given wind speed.

Not all the droplets striking the obstacle, whether supercooled or not, will freeze and be retained on the obstacle. Stallabrass and Hearty (1967) define "icing efficiency" as the product of the collection efficiency

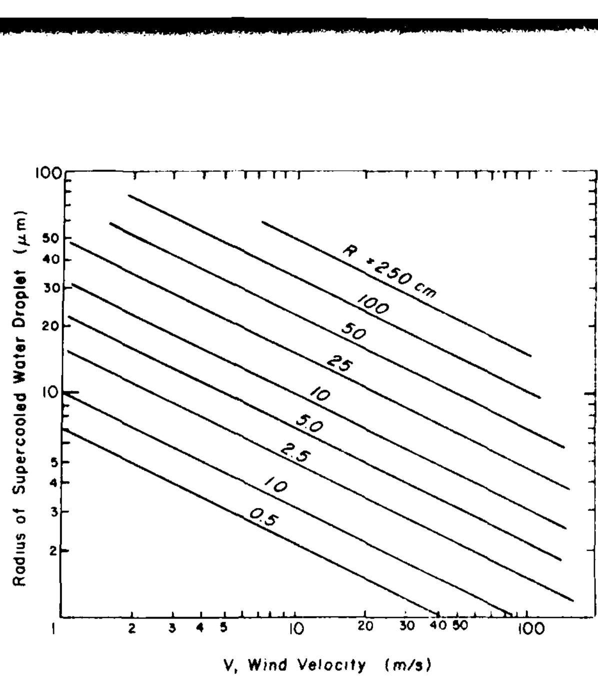

Figure 5. Critical radius of cylinder above which icing theoretically does not occur.

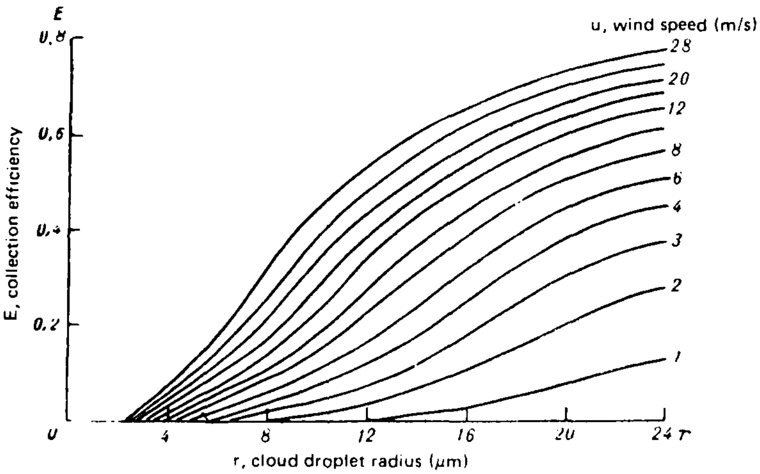

Figure 6. Variation of collection efficiency E *of a 15-mm-radius circular cylinder with cloud droplet radius* r *and wind speed* u *(Glukhov 1972).*

and the freezing fraction. They conducted ice accumulation tests in an icing wind tunnel and measured a one-hour average icing efficiency. The results, some of which are shown in Figure 7, graphically depict the great influences of cylinder diameter and temperature upon ice accretion. (Test conditions were: air speed 50 mph, air temperature between -16° and -5°C, liquid water concentration 3.2 g/m^3, median droplet diameter 200 μm.)

Wind speed influences not only the collection efficiency but also the freezing fraction. With increasing wind speed the icing efficiency (or capture coefficient as it is called in Soviet literature) increases to a maximum and then drops off gradually. The trend, plotted from Soviet observations and shown in Figure 8, results not from a reduction in the collection efficiency but from change in the freezing fraction. (In fact, as is evident from Figure 4, collection efficiency E approaches 1 as K increases, and K is a linearly increasing function of wind speed.) At low wind speeds nearly all the droplets which collide with the surface will freeze because the heat of fusion can be dissipated to the surroundings. As more and more droplets strike the surface with increasing wind speed, however, the heat of fusion cannot be dissipated rapidly enough. Some droplets will remain in the liquid state and

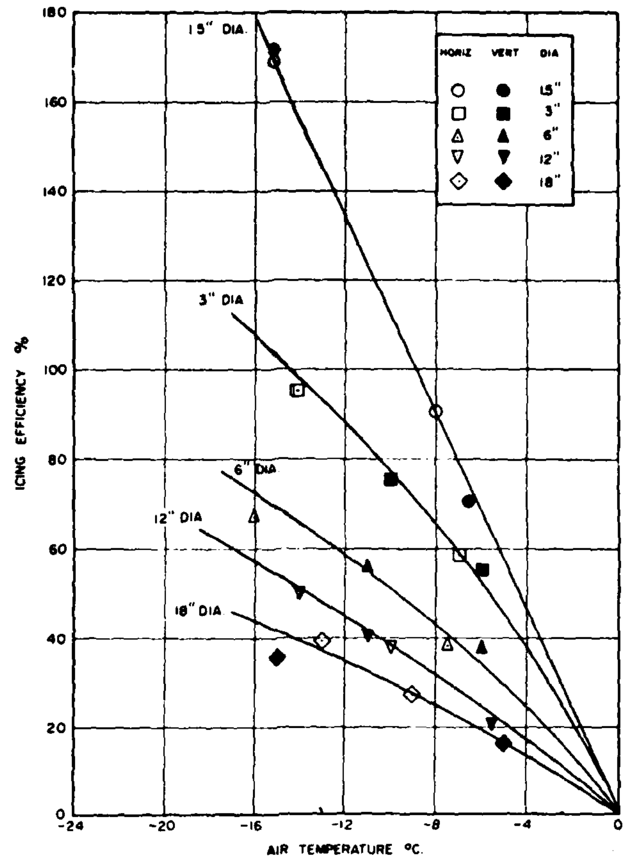

Figure 7. Icing efficiency, i.e. the fraction of water droplets that could strike a cylinder if not deflected and which will freeze on the surface, as related to air temperature and diameter of cylinder. Small cylinders, below 3 in. in these experimental results, will form ice with thickness exceeding the original diameter of the cylinder when temperatures are low enough (Stallabrass and Hearty 1967).

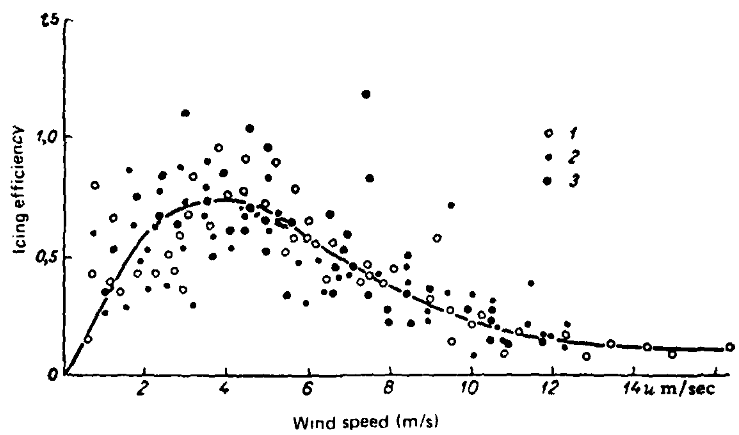

Figure 8. Dependence of icing efficiency (or capture coefficient) on wind speed for various liquid water contents w (Glukhov 1971), where 1) w = 0.12–0.16 g/m^3, 2) w = 0.17–0.21 g/m^3, 3) w = 0.22–0.26 g/m^3.

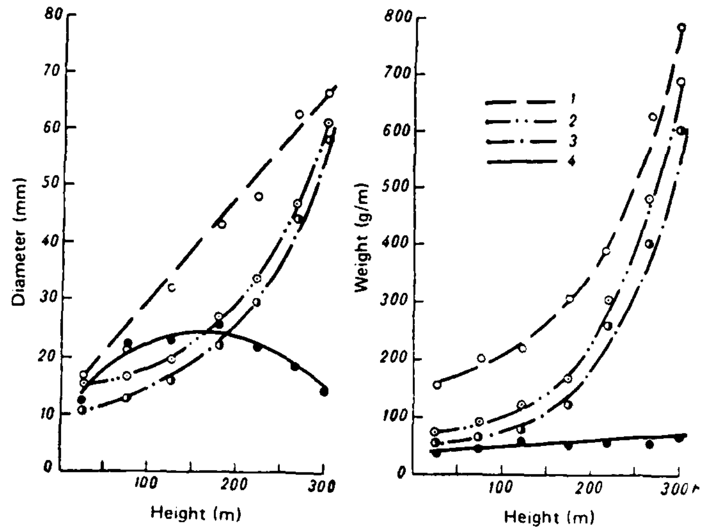

a. Average diameter vs height. *b. Average weight vs height.*

Figure 9. Variation of average diameter and weight of ice accumulation (1—mixture, 2—hard rime, 3—glaze ice, 4—soft rime) with height on meteorological tower at Obninsk, U.S.S.R. (Glukhov 1972).

flow to the periphery, where they are entrained by the air flow and carried away.

b. Effect of height

Both the liquid water content of the air and the wind speed directly affect the accretion rate (see eq 1). Both of these factors also vary with height; LWC varies with cloud type which varies with altitude, and wind speed in the boundary layer generally follows a logarithmic profile, so accretion rates will vary with height. Observations made from a 300-m-high tower in the Soviet Union show the variation of accretion with height for the three types of ice and a mixture (Fig. 9). Frequency of occurrence of the ice types at this same location is given in Table 5.

c. Geographical distribution

Bennett (1959) made a comprehensive search of available data on glaze ice occurrence. Principal sources were railroads, electric power generating and transmission companies, and telephone companies. Most reliable data, therefore, are confined to the continental United States, the populated parts of southern Canada, Europe and Scandinavia. Bennett presents a map made by the U.S. Army Air Force in 1943 which includes Alaska; it shows the mean annual percentage of hourly weather observations with freezing rain or wet snow (Fig. 10). Wet snow was considered as snowfall occurring at temperatures above 32°F and freezing rain was assumed to occur whenever liquid precipitation fell at temperatures ≤ 32°F. The actual occurrence of glaze ice formation will not always follow these conditions. This analysis is of little value in estimating potential ice accretion rates by region and season. The Climatic Atlas of the Outer Continental Shelf Waters and Coastal Regions of Alaska (1977) contains monthly tables of precipitation associated with wind, precipitation types, air temperature (dry and wet bulb), fog, cloud cover, wind speed and direction, and several associated occurrences of these elements. Tattelman and Gringorten (1973) have estimated probabilities of glaze ice storm occurrence according to climatic region, based on data from Bennett (1959). The climatic regions are shown in Figure 11, and probabilities in Tables 6-8. Region VIII incurred no glaze ice storms in the analysis period, but experienced the only two rime ice storms in the country. The National Weather Service does not measure ice accretion, and a climatology of ice accretion is not yet well established, so estimates of icing potential are poor, and any predictive capability for estimating icing severity according to season or geography is meager.

4. Spray icing*

Statistical analysis of more than 3000 cases of ship icing (Borisenkov and Panov 1972) indicates that the principal cause of icing is spray from ocean water (89%). The combined sources of spray and fog, rain, or drizzle accounted for only 6.4% of the cases, and water spray

* This subject is covered in more detail in CRREL Report 77-17 (Minsk 1977).

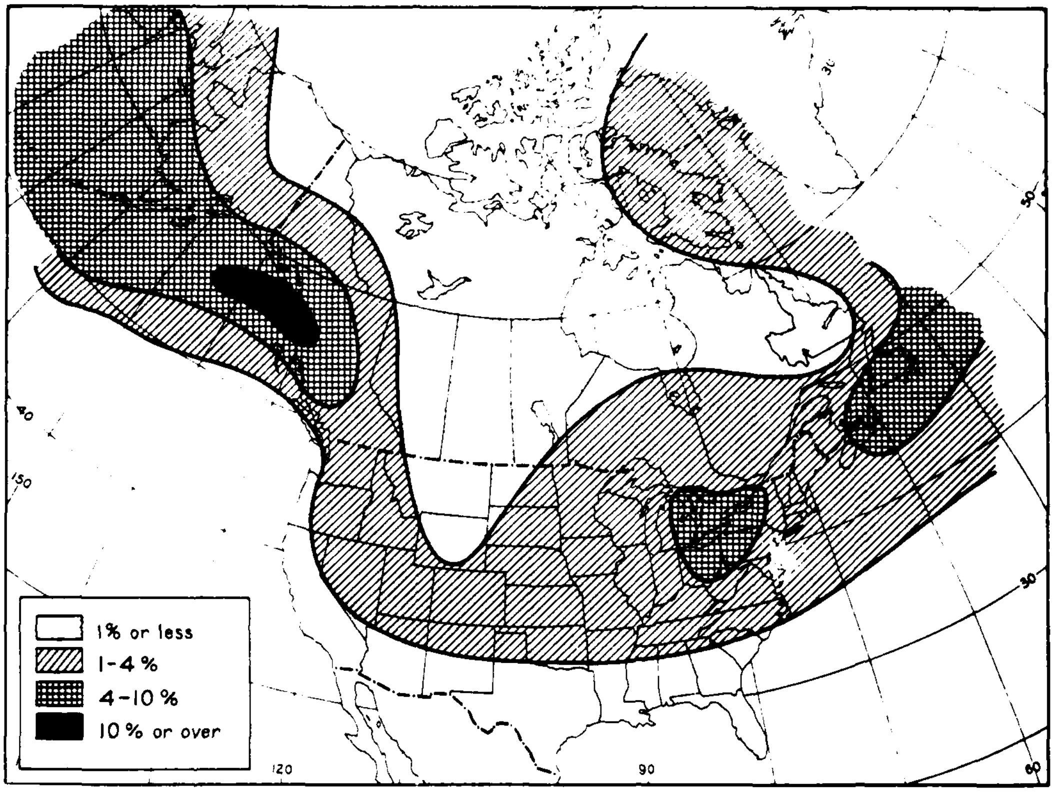

Figure 10. Mean annual percentage of hourly weather observations with freezing rain, North America. Based on a map prepared in 1943 by the Weather Information Service of the U.S. Army Air Forces (Bennett 1959).

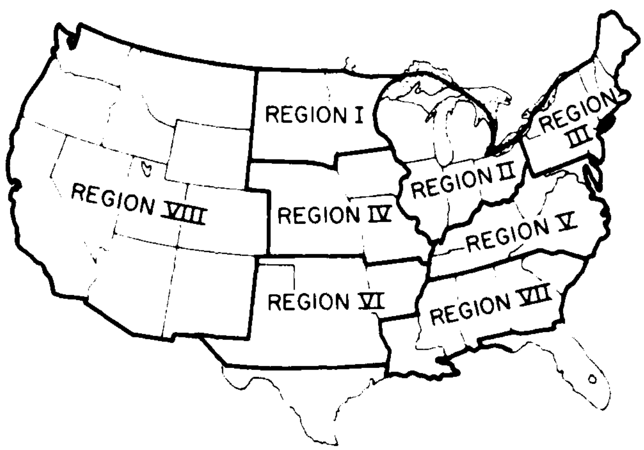

Figure 11. Regions with similar glaze ice characteristics (Tattelman and Gringorten 1973).

Table 5. Occurrence (%) of type of ice by height on meteorological tower in Obninsk, U.S.S.R. (Glukhov 1972).

Height range (m)	Type of ice: Soft rime	Glaze	Hard rime	Mixture
0-100	23	5	5	2
100-200	29	31	25	23
200-300	48	64	70	75
No. of cases	227	237	633	396

Table 6. Probability of at least one occurrence of an ice storm in any year at a representative point in the region (estimated from Bennett 1959, in Tattelman and Gringorten 1973).

Region	Regional Average No. Storms in 9-Year Study	Probability of an Ice Storm (Any Thickness in 1 Year	Regional Average No. Storms ≥ 0.63 cm in 9-Year Study	Probability of an Ice Storm > 0.63 cm in 1 Year	Regional Average No. Storms > 1.25 cm in 9-Year Study	Probability of an Ice Storm > 1.25 cm in 1 Year
I	8	.59	5	.43	3	.28
II	18	.86	7	.54	3	.28
III	20	.89	10	.67	6	.49
IV	15	.81	5	.43	3	.28
V	8	.59	4	.36	2	.20
VI	6	.49	4	.36	2	.20
VII	4	.36	2	.20	0.5	.05

Table 7. Probability of at least one occurrence of an ice storm of stated intensity in any year at a point in the most severe part of the region (estimated from Bennett 1959, in Tattelman and Gringorten 1973).

Region	Regional Maximum No. of Storms in 9-Year Study	Probability of an Ice Storm (Any Thickness) in 1 Year	Regional Maximum No. of Storms >0.63 cm in 9-Year Study	Probability of an Ice Storm >0.63 cm in 1 Year	Regional Maximum No. of Storms > 1.25 cm in 9-Year Study	Probability of an Ice Storm > 1.25 cm in 1 Year
I	24	.93	14	.79	8	.59
II	35	.98	10	.67	4	.36
III	44	.99	19	.88	9	.63
IV	35	.98	11	.71	8	.59
V	20	.89	9	.63	6	.49
VI	16	.83	8	.59	5	.43
VII	11	.71	4	.36	4	.36

Table 8. Number of ice storms > 2.5 cm and > 5 cm in 50 years and the probability of at least one occurrence in one year in the most severe state in each region (Tattelman and Gringorten 1973).

Region	Number Ice Storms ≥ 2.5 cm in 50 Years	Probability of an Ice Storm ≥ 2.5 cm in 1 Year	Number Ice Storms > 5 cm in 50 Years	Probability of an Ice Storm ≥ 5 cm in 1 Year
I	4	.08	2	.04
II	8	.15	2	.04
III	8	.16	3	.06
IV	4	.08	2	.04
V	2	.04	1	.02
VI	4	.08	1	.02
VII	3	.06	1	.02

Table 9. Distribution of ice incidence (%) for Soviet ships in various seas as related to air and water temperatures (Borisenkov and Pchelko 1972).

	Air temperature (°C)					Water temperature (°C)					
Sea	[illegible]	[illegible]	-10.1-15.0	-15.1-20.0	No. of cases	-2.0-1.1	-1.0-0.0	0.1+3.0	3.0+6.0	+6.0	No. of cases
Bering Sea	15	60	23	2	560	6	6	78	10		517
Sea of Okhotsk	19	64	12	5	340	20	26	50	4		297
Sea of Japan and Tatarskiy Strait	13	54	27	6	201	15	14	52	4	4	192
Western Pacific Ocean	2	65	10		281	16	19	55	10		239
Barents Sea Norwegian Sea	[illegible]	2	36	1	663	2	3	45	49	1	573
Baltic Sea	[illegible]	[illegible]	41		46		11	89			36
Labrador region	21	55	18	6	90	11	32	49	8		82
Black Sea and Sea of Azov	2	36	4		22		24	48	28		21

and snow only 1.1 [illegible]. The cases of icing attributable only to fog, rain or drizzle account for 2% [illegible]. Tables 9 and 10 (from Borisenkov and Pchelko 1972) show the distribution of icing occurrences for various regions as a function of air and water temperatures, wind speed and direction, and wave height.

Icing rarely occurs at air temperatures above 6°C, and has been recorded at temperatures below -25°C. Shekhtman (1968) has related ice accretion rate with wind speed; his analysis is summarized in Table 11. Research in Japan (Tabata et al. 1963) has also related icing severity with air temperature and wind speed (Fig. 12). Three classes of icing (none, significant, and heavy) correspond to the Soviet growth rate classification in Table [illegible]. In general, [illegible] [illegible] [illegible]

Ice thickness reached 20 cm in 50% of the cases. Deck accumulation from spray and snowfall reached a maximum of 100 cm.

Soviet experiments and observations over three winters on ships in the Sea of Japan, Barents Sea and Baltic Sea established ranges of icing activity (Borisenkov and Pchelko 1972). Air temperatures down to -3°C were not accompanied by significant icing. At relatively low wind speeds (7-10 m/s) and air temperatures below -3°C, the bow of the ship becomes iced. The rest of the ship accretes only slight amounts of ice, or does not accumulate any at all. Strong winds (15-25 m/s) and air temperatures to -15°C result in ice accretion on the main deck, rigging, mast and spars, bow companionway, and bridge. Maximum deposition occurs on the main deck and trawling winch. The upper bridge and the boat deck accumulate very little ice. The ship's

Table 10. **Distribution of icing incidence (%) for Soviet ships in various seas as related to wind direction and wave height (Borisenkov and Pchelko 1972).**

Sea	*Wind direction and speed (m/s)* 271-360° <10	>10	00-90° <10	>10	91-180° <10	>10	181-270° <10	>10	*No. of cases*	*Wave height (m)* 1-3	>3	*No. of cases*	*Period of ships' icing*
Bering Sea	12	43	16	23	1	1	2	2	567	55	45	484	Oct-Mar
Sea of Okhotsk	19	34	3	10	1	3	10	20	323	73	27	257	Oct-Mar
Sea of Japan and Tatarskiy Strait	23	55	5	9			1	7	199	82	18	151	Dec-Feb
Western Pacific Ocean	15	52	1	8	1	2	6	15	232	71	29	185	Nov-Feb
Barents Sea, Norwegian Sea	2	9	7	14	19	20	9	20	638	78	22	525	Dec-Mar
Baltic Sea		24		32	22		22		45	79	21	45	Jan-Mar
Labrador region	21	48	2	2	1	2	12	12	87	67	33	43	Dec-Feb
Black Sea and Sea of Azov	55			45					11				Jan-Mar

Table 11. **Frequency (%) of ice intensity related to wind speed (Shekhtman 1968).**

Icing intensity	*Wind speed (knots)* 0-2	3-10	11-20	21-29	30 and over	*Avg. speed (knots)*	*No. of cases*
Fast growth	2	4	12	42	40	29	15
Slow growth	1	8	29	43	19	23	303
No change	2	22	39	24	13	17	54

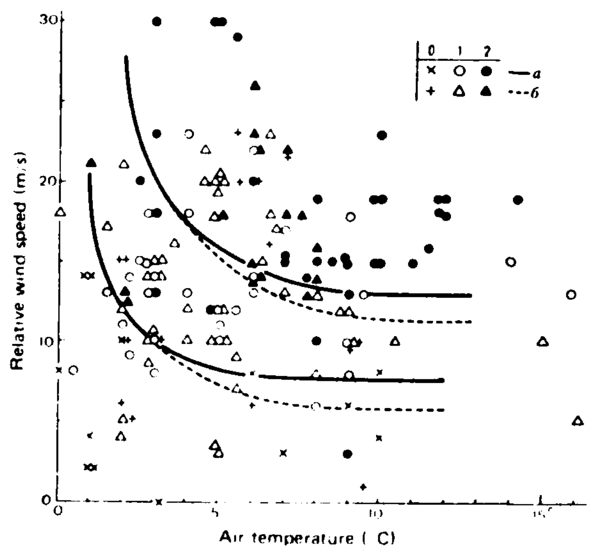

Figure 12. Icing severity as related to air temperature and wind velocity (Borisenkov and Panov 1972, taken from Japanese data in Tabata et al. 1963) where a = 450-ton displacement ship; b = 350-ton displacement ship; 0 = no icing; 1 = significant icing; 2 = heavy icing.

stern does not become iced even when the heading is downwind.

The distribution of ice over a ship tends to be erratic. Investigations on the *Professor Somov* in January-February 1968 established the following pattern of ice distribution: 30–70% on the horizontal surfaces, 15–40% on the vertical surfaces, 5–30% on the surfaces of complex configuration (instruments and equipment), and 0–30% on the round surfaces such as mast, spars, and rigging. In the presence of spray, ice accretion commences immediately at temperatures below -3°C on the metal surfaces of the ship and on canvas equipment covers. However, ice does not form immediately on the wood decks; instead, a slush develops which mixes with seawater and flows overboard through the freeing ports. For a period of 1½ to 2 hours after formation on metal and canvas surfaces the ice is loosely bonded and can be easily knocked or scraped off. After that time the ice becomes tightly bonded to the surfaces and can be removed only with great difficulty.

Shellard (1974) summarizes conditions for icing due to seawater. These occur whenever sea spray is present at the same time that the air temperature, and therefore the temperature of most exposed surfaces, is below the freezing point of seawater. The freezing point will vary from a little below 0°C for only slightly saline waters to -1.9°C for ocean water. A small vessel is likely to begin generating spray in a sea corresponding to force 5 (17-21 knots); at force 6 (22-27 knots, with wave heights of 3 m or more) most small vessels moving against the waves will be showered in spray. Spray blown from wave tops is not likely to become a serious source of icing, however, until much higher wind speeds are reached, because such spray is patchy and at a low level when it begins to appear at 17-27 knots. As a consequence, large amounts will not likely reach deck level until at least force 9 (41–47 knots), the point at which visibility begins to be affected. These observations can be applied to fixed installations which may not generate quantities of the larger droplets from impacting waves.

Woodcock (1953) reports that foam patches resulting from whitecaps at the sea surface remained visible from an aircraft for more than two minutes in a force 5 wind in the Hawaiian area, which supports Shellard's comment regarding the initiation of spray icing at that wind speed.

5. Structural design factors

a. Dead loads

Freezing rain falling under calm or low wind speed conditions will coat horizontal surfaces with ice; the windward side of a structure will also accrete ice on surfaces oriented other than horizontally, both from runoff water freezing slowly because of high rainfall rates, and by direct contact of supercooled water droplets on the sloping or vertical surface.

A relationship between the precipitation measured by a precipitation gage and ice that will accrete on a vertical surface (assuming necessary negative temperatures prevail) has been proposed by McKay and Thompson (1969):

$$T = 0.785\ VP^{0.88} \qquad (3)$$

where T = rate of precipitation striking a vertical surface, in./hr
V = wind speed, mph
P = precipitation rate, in./hr

This relationship assumes that the collection efficiency E is unity.

Loads due to ice accretion are generally less than design snow loads, but the prevalence of structural collapse of antenna towers, powerline cables and support structures under conditions of no wind suggests that ice loads can be high. For example, a glaze storm on 27-29 January 1940 struck Great Britain and resulted in some of the greatest accumulations of ice ever recorded: 6 in. of ice on an automobile and 4 in. on twigs in Worcestershire, and a 2.4-in.-diameter accumulation on a telegraph wire in Wiltshire. The maximum thickness reported in a series of observations in the Soviet Union in the 1920's was a diameter of 114 mm on a 5-mm wire in Tokmak in the Kirghiz (Bennett 1959). Ice that accumulated to a diameter of 25 cm on guy wires of a tower in Newfoundland was estimated to have weighed over 40 kg/m (Boyd and Williams 1968). Tables 12 and 13 present estimates of ice accumulation on a cylinder for the regions defined in Figure 11 (Tattleman and Gringorten 1973). These values are based on 61 storms and required subjective development and manipulation of the statistics. Caution is required in applying these estimates in design.

b. Wind field in the boundary layer

Wind speed in the lower atmosphere varies with height as a consequence of the frictional drag developed by the rigid surface on the flow. It has been found that a logarithmic decay expresses this change quite closely:

$$\bar{u}_z = (u_*/k)\ \ln (z/z_0) \qquad (4)$$

where u_z = wind speed at height z
u_* = friction velocity
k = von Karman's constant (≈0.40)
z_0 = roughness length (height at which the neutral wind profile extrapolates to zero wind speed)

Table 12. Ice thickness, estimated to the nearest 0.1 cm, for different return periods, at a representative point (AVG), and at a point in the most severe location (MAX) for each region (Tattelman and Gringorten 1973).

	Return Period (Years)											
	2		5		10		25		50		100	
Region	AVG	MAX	AVG	MAX	AVG	MAX	AVG	MAX	AVG	MAX	AVG	MAX
I	0.4	1.4	1.4	2.1	1.6	2.4	1.8	5.0	1.9	7.1	2.1	>7.5
II	0.7	1.0	1.4	2.1	1.7	3.3	2.0	5.0	2.2	6.0	2.4	7.0
III	1.2	1.6	1.6	2.4	1.8	3.8	2.0	5.8	2.1	7.2	2.3	>7.5
IV	0.5	1.4	1.4	2.1	1.6	2.4	1.8	5.0	1.9	7.2	2.1	>7.5
V	0.2	1.2	1.2	1.8	1.5	2.2	1.7	2.5	1.8	5.0	2.0	7.0
VI	0	1.0	1.2	1.9	1.5	2.4	1.7	3.8	1.9	5.0	2.1	6.0
VII	0	0.4	0.6	1.8	1.0	2.2	1.3	3.4	1.5	5.0	1.7	6.3

Table 13. Ice thickness, estimated to the nearest 0.1 cm, combined with wind gusts > 20 m/s in the most severe location in each region (Tattelman and Gringorten 1973).

	Return Period (Years)		
Region	25	50	100
I	2.5	5.0	6.5
II	3.7	5.0	6.5
III	2.6	5.0	6.6
IV	<2.5	3.5	5.6
V	<2.5	<2.5	3.6
VI	<2.5	3.0	4.5
VII	<2.5	2.5	4.1

u_* can be calculated using the relationship that the slope of the ln z vs u plot is $k\ u_*$. It increases with roughness of surface and with mean wind speed, but it is approximately equal to u/10.

Some values of z_0 in feet are:

water 3×10^{-6} to 3×10^{-4}
ice 3×10^{-5}
snow 2×10^{-4} to 3×10^{-3}

Measurement of wind speed at one height enables calculation of the speed at another height:

$$u_z = u_r \frac{\ln (z/z_0)}{\ln (z_r/z_0)} \qquad (5)$$

where u_z = wind speed at height z

u_r = measured wind speed at reference height z_r
z_0 = roughness length.

c. Wind loads

The American National Standard Building Code (ANSI 1972) states that wind loads on buildings and other structures shall be determined by selecting a mean recurrence interval based on usage, anticipated structure life, sensitivity to wind, and life or property risk in case of failure. A basic wind speed is selected, based on annual extreme fastest-mile speed 30 ft above ground for either a 50- or 100-year mean recurrence interval (using a published small scale map if good local data are not available). Then the selected basic wind speed is converted to effective velocity pressures q_F for buildings and structures and q_P for parts and portions of structures, at various heights, defined as

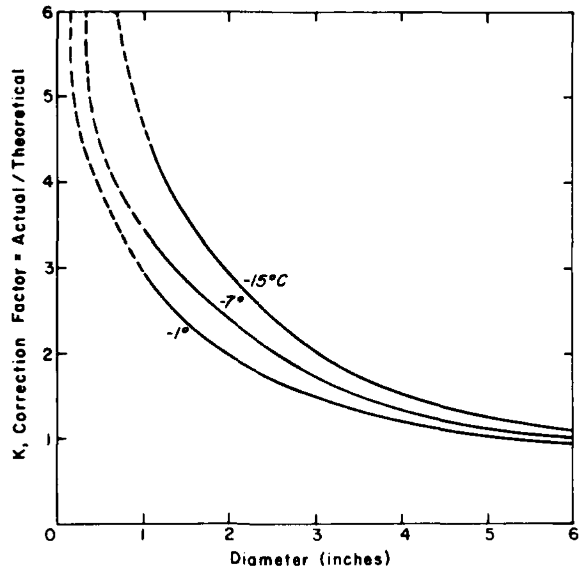

Figure 13. Correction factor K, for use in estimating radial ice thickness (Chainé and Castonguay 1974).

$$q_F = K_z\, G_F\, q_{30}$$

and

$$q_P = K_z\, G_P\, q_{30}$$

where K_z = velocity pressure coefficient dependent on type of exposure and height z above ground
G_F, G_P = gust factors dependent on type of exposure and dynamic structural response
q_{30} = basic wind pressure (lb_f/ft^2) = $0.00256\, V_{30}^2$, where V_{30} = basic wind speed in mph.

Tables of q_F and q_P are included in ANSI A58.1 (ANSI 1972). A procedure is also given for calculation of gust factors. The National Building Code of Canada (National Research Council 1977) also includes sections on wind effect, wind levels, and icing factors.

Chainé and Skeates (1974) have prepared tables showing ice accumulation on a horizontal surface and the related vertical surface accumulation, based on observed maximum wind speed and computed gust speeds, and the equivalent radial accretion, transverse wind loading and wind pressure on a cable and tower. Nearly 150 locations in Canada are tabulated.

The maximum computed gust is calculated from

$$G_m = 5.8 + 1.29\, V_m \qquad (8)$$

where V_m = maximum wind speed, mph.

The wind pressure coefficients for flat and cylindrical surfaces were calculated from

flat surfaces: $P_f = 0.0042\, G_m^{\,2}$ lb/ft² (9)

cylindrical surfaces: $P_c = 0.0026\, V_m^{\,2}$ lb/ft² (10)

where G_m and V_m are given above.

Equivalent radial thickness A_r is defined by Chainé as the probable ice that would accrete uniformly around a 1-in.-diameter cylinder equivalent to the asymmetric natural formation:

$$A_r = \left[\frac{rK}{2}\left(A_h^{\,2} + A_v^{\,2}\right)^{1/2} + r^2\right]^{1/2} - r \qquad (11)$$

where

K = correction factor based on cylinder size = $\dfrac{\text{actual accumulation}}{\text{theoretical accumulation}}$

A_h = accumulation on horizontal surface
A_v = accumulation on vertical surface
r = cylinder radius

The correction factor K is the ratio of experimentally measured ice thickness to theoretical ice thickness. Chainé has prepared a graph of this factor as a function of accreting cylinder diameter and air temperatures (Fig. 13). The experimental measurements were those made by Stallabrass and Hearty (1967) for a very limited range of conditions (they measured the accumulation after a one-hour exposure to wind of 50 mph and liquid water content of 3.2 g/m^3 and a median volume diameter of droplets of about 200 μm). This equation is therefore only a guide and not to be accepted as a precise determination of expected ice thickness.

An approximate relationship between accumulation on vertical and horizontal surfaces was developed by Chainé and Castonguay (1974):

$$A_v = A_h V/10 \qquad (12)$$

Transverse wind loading L_c as used by Chainé gives the maximum load on a cable (powerline) occurring during an ice storm as a combination of ice accumulation and wind; it is calculated by

$$L_c = 0.0026 \, V_m^2 \, \frac{d + 2A_r}{12} \ \text{lb/ft} \qquad (13)$$

where

d = conductor diameter, in.
A_r = equivalent radial thickness, in.

6. Techniques for minimizing structural icing

No completely effective methods of ice accretion control or removal have been found. Mechanical (impaction) methods are the most common techniques, but experiments have been conducted utilizing heated surfaces, icephobic surfaces, deformable surfaces, and freezing point depressants. Also, no device for unequivocal remote measurement of ice accumulation rate is available, though some techniques are available for such measurements under experimental conditions. In critical areas, where no ice accumulation can be accepted, or where accumulation beyond a certain point may lead to catastrophic failure, active control methods must be used. Application of heat is the most dependable but not necessarily the most convenient, practicable, or cost-effective method, because irregular surfaces, surfaces exposed to very high heat losses, and extensive areas all present problems.

Methods of removal of ice accumulations reported in the literature are conventional: baseball bats, sledge hammers, axes, hammers, picks, and other impact instruments are frequently mentioned as the only tool available, but icephobic coatings and heated surfaces have been experimented with. By itself, an icephobic or low-energy surface may be insufficient to reduce ice accumulation, but in association with some other mechanism such as vibration or a deformable surface ice removal may be accomplished effectively. Vibration or deformation alone is usually insufficient to remove well-bonded ice.

A poly(dimethylsiloxane)-bisphenol-A-polycarbonate block copolymer developed for CRREL (Jellinek 1978) has been used successfully to reduce the adhesion of ice to navigation lock walls (Frankenstein et al. 1976). The same material has been applied to a dish radar antenna to reduce heat input necessary to control ice accumulation (Hanamoto 1980); tests showed that the 145 minutes required to eliminate 0.64 cm (0.25 in.) of ice on the antenna surface heated at 2.3 W/m^2 at an air temperature of −2.5 C could be reduced to 20-44 minutes. Vibration of the coated, unheated surface did not eliminate the ice accumulation. An organic freezing point depressant, Monsanto Santomelt 990-CR was effective in keeping the flight deck, turnbuckles, shackles, and lines clear of ice on the USCGC Burton Island (Bates 1973). The use of and search for additional effective icephobic surface treatments are discussed by Sayward (1979).

Stallabrass (1970) investigated a number of methods of reducing accretion of ice on ships. The methods utilized, in order of their deicing effectiveness or ease of ice removal, were:

1. Pneumatic deicer
2. Freezing point depressant (ethylene glycol)
3. Rubber-surfaced plastic foam on steel panel
4. Gray deck paint on wooden panel
5. Spar varnish on wooden panel
6. Bare polyethylene foam on steel panel
7. Black rust-preventive paint on steel panel
8. Gray deck paint on steel panel

These qualitative tests were made in an icing wind tunnel and on outdoor (land) test sites. In addition, a polyethylene-sheathed parallel filament rope was compared with a steel cable for ice accretion and removal. Because of the lower torsional stiffness of the rope, it tended to twist during the icing event and ice accreted around the entire circumference, in contrast to the steel cable which presented a constant face to the airborne droplets and therefore accumulated ice asymmetrically. Little difference was noted in the ease of removal of ice from polyethylene-sheathed rope compared to the steel cable because of the encapsulation of the plastic.

The 4 x 3 ft pneumatic deicer worked effectively when attached to both a 1-ft-diameter cylindrical form simulating a mast and when spread flat on a panel.

Because small diameter cylinders accumulate more ice than large diameter cylinders, accretion can be reduced by gathering together and enclosing a number of small cables in a sheath, or installing a large diameter sheath around a single small cable. A British-designed ice-resistant trawler uses large diameter unguyed tripod masts, rather than a single mast guyed by multiple rigging cables, as a means of reducing sail area and the amount of superstructure icing potential.

An item in a popular Soviet publication (*Soviet Life* 1975) reports that their scientists have suggested the use of an anti-icing "shirt" for protection against ship icing, and that tests have proved the effectiveness of the method. It is quite likely that this is merely a flexible plastic sheeting covering portions of the superstructure.

Ice and snow accumulation on power line towers in Norway has been reduced by enclosing monolithic concrete structures as well as open-lattice steel towers with sheets of solid, corrugated plastic. This technique may be applicable to ocean installations.

Since sea spray is the principal source of icing in maritime regions, reduction of the supply of spray from breaking waves is an obvious control strategy for fixed installations. Wave damping would be required for the maximum distance that a droplet would travel. Large (1 to 3.5 mm) droplets generated by wave impaction, rather than spray whipped off breaking swell waves, are of primary concern. Droplet size of the latter averages 200 μm (Wu 1973). Borisenkov and Panov (1972) state that the flight time of droplets generated by a ship plowing into waves is 1.3–1.4 s until impact on the ship. Since this presumably is the forward part of the ship, total flight time until the drop reaches the sea again is reasonably estimated as 6 s. In a 30-m/s wind, a drop would travel 180 m. A small droplet, 200 μm and below, would travel a much longer distance. It is not likely that it would be economical to install wave damping for such a large area.

Deflection of droplets from the trajectory that will carry them to a surface to be protected may be possible. This may be accomplished by an air curtain, or by another surface whose shape can be given optimum aerodynamic design or which may be permitted to accumulate ice. This approach is experimental and requires design for specific conditions.

Heated water is used for flushing decks and other surfaces for ice removal. However, large quantities of seawater even slightly above the freezing point can be used for removal or protection if cooling due to wind is not excessive and if proper drainage is provided to prevent ponding.

7. Data collection needs

Geographical, seasonal, and altitudinal distribution of icing is poorly known and at present the National Weather Service reporting network makes no observations or measurements of ice accretion. The occurrence of freezing or frozen precipitation is reported, but there is only a loosely defined relationship between ice formation and the amount of precipitable water, as was discussed in Section 5a. The NWS has considered including direct measurement of ice accretion in an automatic weather sensing apparatus and tested the Rosemount ice detector as a candidate. This instrument, an automatic continuous-recording device (Rosemount Inc., Minneapolis), was developed initially for measurements on aircraft, but has been adapted for detection and measurement of land structure icing. Detection is based on the change in resonant frequency of a small vibrating rod in the droplet stream. Sensitivity can be selected to initiate a deicing cycle when ice growth has reached a predetermined mass; the number of deicing cycles is a measure of accumulation rate.

The most comprehensive data on altitudinal variation of icing have resulted from the two Soviet instrumented towers. A Soviet network of cable icing measurements has also been established to measure the accumulation on a standard diameter cable (5 mm), though other diameters are also used in order to determine the collection efficiency variation with cable size and with meteorological conditions. A similar icing accretion reporting network in Alaska and other northern states would provide much useful data. The construction of instrumented towers with provisions to measure ice accretion variation with elevation, and associated means to measure cloud liquid water content and droplet size at a limited number of locations, would provide the basis for establishing a predictive capability.

8. Literature cited

American National Standards Institute (1972) American National Standard building code requirements for minimum design loads in buildings and other structures. American National Standards Institute, New York, N.Y., ANSI A58.1-1972.

Anon. (1962) Precipitation measurements at sea. World Meteorological Organization, Geneva, Switzerland, Technical Note No. 47.

Bates, C.C. (1973) Navigation of ice-covered waters: Some new initiatives by the United States of America. In *23rd Report, International Congress of Navigation.* Permanent International Association of Navigation Congresses, Brussels.

Bennett, I. (1959) Glaze, its meteorology and climatology, geographical distribution, and economic effects. Quartermaster Research and Engineering Center, Technical Report EP-105.

Borisenkov, E.P. and I.G. Pchelko (Ed.) (1972) Indicators for forecasting ship icing (in Russian). Arkticheskii i Antarkticheskii Nauchno-issledovatel'skii Institut, Leningrad. Also CRREL Draft Translation 481, AD 030113.

Borisenkov, E.P. and V.V. Panov (1972) Basic results and perspectives on the investigation of hydrometeorological conditions related to ship icing (in Russian). Arkticheskii i Antarkticheskii Nauchno-issledovatel'skii Institut, Leningrad, Trudy, vol. 298, p. 5-33. Also CRREL Draft Translation 411. AD A003215.

Borovikov, A.M. et al. (1961) *Physics of Clouds* (in Russian). Leningrad: Gidrometeoizdat.

Boyd, D.W. and G.P. Williams (1968) Atmospheric icing of structures. Division of Building Research, National Research Council, Ottawa, Canada, Technical Paper 275.

Butkovich, T.R. (1954) Ultimate strength of ice. U.S. Army Snow, Ice and Permafrost Research Establishment (SIPRE) Research Report 11. AD 050514.

Chainé, P.M. and G. Castonguay (1974) New approach to radial ice thickness concept applied to bundle-like conductors. Atmospheric Environment, Environment Canada, Toronto.

Chainé, P.M. and P. Skeates (1974) Ice accretion handbook (freezing precipitation). Industrial Meteorology—Study VI. Atmospheric Environment, Environment Canada, Toronto.

Frankenstein, G., J. Wuebben, H.H.G. Jellinek and R. Yokota (1976) Ice removal from the walls of navigation locks. *Proceedings of Symposium on Inland Waters for Navigation, Flood Control and Water Diversion*, Colorado State University, August 10-12.

Glukhov, V.G. (1971) Evaluation of ice loads on high structures from aerological observations (in Russian). Gidrometeoizdat, Trudy, vol. 283, GGO, p. 3-11. (Translation: *Soviet Hydrology, Selected Papers*, Issue no. 3, 1971, p. 223-228.)

Glukhov, V.G. (1972) Meteorological conditions for formation of ice on high structures (in Russian). Gidrometeoizdat, Trudy, vol. 311, GGO.

Hanamoto, B., J.J. Gagnon and B. Pratt (1980) Deicing a satellite communication antenna. CRREL Special Report 80-18. ADA 085397.

Houghton, H.G. and W.H. Radford (1938) On the measurement of drop size and liquid water content in fogs and clouds. M.I.T. Papers on Physical Oceanography and Meteorology.

Jellinek, H.H.G., H. Kachi, S. Kittaka, M. Lee and R. Yokota (1978) Ice releasing block-copolymer coatings. *Colloid and Polymer Science*, vol. 256, p. 544-551.

Kocmond, W.C., R.J. Pilié, W.J. Eadie, E.J. Mack and R.P. Leonard (1971) Investigation of warm fog properties and fog modification concepts. NASA CR-1731, National Aeronautics and Space Administration, Washington, D.C.

Kuroiwa, D. (1965) Icing and snow accretion on electric wires. CRREL Research Report 123. AD 611750.

Langmuir, I. and K. Blodgett (1946) Mathematical investigation of water droplet trajectories. U.S. Army Air Force Technical Report 5418.

McKay, G.A. and H.A. Thompson (1969) Estimating the hazard of ice accretion in Canada from climatological data. *Journal of Applied Meteorology*, vol. 8, no. 6, p. 927-935.

Minsk, L.D. (1977) Ice accumulation on ocean structures. CRREL Report 77-17. ADA 044258.

National Research Council (1977) National Building Code of Canada 1977, NRCC No. 15555. Climatic Information for Building Design in Canada 1977. Supplement No. 1 to the National Building Code of Canada, NRCC No. 15556. Commentary B, Wind Loads. Commentaries on Part 4 of the National Building Code of Canada 1977. Supplement No. 4 to the National Building Code of Canada, NRCC 15558. National Research Council of Canada, Ottawa.

Pilié, R.J. and W.C. Kocmond (1967) Project fog drops. Cornell Aeronautical Laboratory, NASA CR-675. National Aeronautics and Space Administration, Washington, D.C.

Sayward, J.M. (1979) Seeking low ice adhesion. CRREL Special Report 79-11. ADA 071040.

Searby, H.W., J.L. Wise, W.A. Brower, Jr., H.F. Diaz and A.S. Prechtel (1977) Climatic atlas of the outer continental shelf waters and coastal regions of Alaska. Vol. 1, Gulf of Alaska; Vol. 2, Bering, Sea; Vol. 3, Chukchi–Beaufort Sea. Arctic Environmental Information and Data Center Publication B-77, University of Alaska.

Shekhtman, A.N. (1968) The probability and intensity of the icing-up of ocean-going vessels (in Russian). Nauchno-issledovatel'skii Institut Aeroklimatologii, Moscow, Trudy, vol. 50, p. 55-65.

Shellard, H.C. (1974) The meteorological aspects of ice accretion on ships. World Meteorological Organization, Geneva, Marine Science Affairs Report no. 10 (WMO-No. 397).

Stallabrass, J.R. (1970) Methods for the alleviation of ship icing. National Research Council, Ottawa, Canada, Mechanical Engineering Report MD-51.

Stallabrass, J.R. and P.F. Hearty (1967) The icing of cylinders in conditions of simulated freezing sea spray. National Research Council, Ottawa, Canada, Mechanical Engineering Report MD-50, NRC no. 9782.

Tabata, T., S. Iwata and N. Ono (1963) Studies on the ice accumulation on ships. I. *Low Temperature Science*, series A, vol. 21, p. 173-221.

Tattelman, P. and I.I. Gringorten (1973) Estimated glaze ice and wind loads at the earth's surface for the contiguous United States. Air Force Cambridge Research Laboratories Report No. AFCRL-TR-73-0646, L.G. Hanscom Field, Bedford, Mass.

Weickmann, H.K. and H.J. aufm Kampe (1953) Physical properties of cumulus clouds. *Journal of Meteorology*, vol. 10, no. 3, p. 204-211.

Woodcock, A.H. (1953) Salt nuclei in marine air as a function of altitude and wind force. *Journal of Meteorology*, vol. 10, no. 5, p. 362-371.

A facsimile catalog card in Library of Congress MARC format is reproduced below.

Minsk, L.D.
Icing on structures / by L.D. Minsk. Hanover, N.H.: U.S. Cold Regions Research and Engineering Laboratory; Springfield, Va.: available from National Technical Information Service, 1980.
iv, 22 p., illus.; 28 cm. (CRREL Report 80-31.)
Prepared for Office of Marine Geology, U.S. Geological Survey by Corps of Engineers, U.S. Army Cold Regions Research and Engineering Laboratory.
Bibliography: p. 17.
1. Deicing materials. 2. Deicing systems. 3. Ice. 4. Ice accretion. 5. Ice loads. 6. Ice prevention. I. United States. Army. Corps of Engineers. II. Army Cold Regions Research and Engineering Laboratory, Hanover, N.H. III. Series: CRREL Report 80-31.

U.S. GOVERNMENT PRINTING OFFICE: 1981 700-660/309

DA

FILM

3 –